Supporting Information

Auxeticity of monolayer, few-layer, vdW heterostructure and ribbon penta-graphene

Viet Hung Ho[1], Duc Tam Ho[2], Won Ho Shin[1], Sung Youb Kim[1,*]

[1] Department of Mechanical Engineering, Ulsan National Institute of Science and Technology, Ulsan 44919, South Korea

[2] Department of Mechanical and Construction Engineering, Northumbria University, Newcastle upon Tyne NE1 8ST, United Kingdom

*Corresponding author's e-mail: sykim@unist.ac.kr

Out-of-plane Poisson's ratio few-layer penta-graphene

In section 3.1, we showed that monolayer PG has a positive out-of-plane Poisson's ratio (Fig. 2). In this part, we investigated the out-of-plane Poisson's ratio of few-layer PG. Firstly, the deformation of bulk AA- and AB-T12C under tension was examined. Fig. S5a shows the reduction of out-of-plane Poisson's ratio of bulk AA- and AB-T12C under tension along the *x*-direction. For AA-T12C, ν_{xz} gradually decreased from 0.174 to 0.117, which were obtained at $\varepsilon = 0$ and $\varepsilon = 0.16$, respectively. For AB-T12C, ν_{xz} decreased from 0.089 at $\varepsilon = 0$ to zero value at $\varepsilon = 0.117$. After the applied strain excess 0.117, the value of ν_{xz} becomes negative, which indicates the out-of-plane auxeticity. To explain the insight of auxeticity, we analyzed the change of height (Δh) and interlayer distance (Δd) under stretching (Fig S3b). Owing to the structure of few-layer PG, C_2 atoms on the lower layer were pulled downward, whereas C_2 atoms on the lower layer were pulled upward (Fig.S5c), causing the elongation of the interlayer distance. Therefore, the interlayer distance increased and resulted in a negative contribution to ν_{xz}. In the opposite tendency with Δd, the variation of Δh decreased owing to the reduction of θ_1 and θ_2. Moreover, the reduction of Δh in few-layer PG was smaller when compared to the that of monolayer PG. It can be explained that the interlayer bond of C_2 between layers may

limit the movement of C_2 atoms along the *z*-direction. From Fig. S5b, it was also possible to observe that the amount of reduction of Δh in the case of AA-T12C was larger when compared to that of AB-T12C. Moreover, in the case of AB-T12C, the reduction of Δh became smaller as the structure was stretched. Therefore, along with the enhancement of Δd, the negative out-of-plane Poisson's ratio was obtained in AB-T12C and few-layer PG with AB stacking configuration. Furthermore, Fig. S5d shows the strain dependence of ν_{xz} of AB stacking PG with 12, 14, and 16 layers. Thus, it showed that ν_{xz} and ε_c tends to decrease with the increase of layers.

Dependence of warped edge on wavelength

We discuss the relationship between the characteristics of the warped edge and wavelength. To do that, we study four models of PR ribbon with different lengths (*L*) in the *y*-direction: 359.23 Å, 431.08 Å, 466.70 Å, and 516.92 Å, while the width of ribbons (*w*) is 143.69 Å. For each model, the number of warps can be changed from 4 to 12. As a result, the half wavelength (λ) of ribbon varies from 25.67 Å to 77.80 Å. Fig. S9 shows the dependence of edge energy of the ribbon on the half wavelength. The edge energy can be expressed as:

$$E_e = \frac{E_r - E_m}{2L}$$

where E_e, E_r, and E_m energy of edge, PG ribbon, and monolayer PG (without edge), respectively; while *L* is the length of ribbon in the *y*-direction. We obtain that the edge energy reaches a robust valley point when the half wavelength is approximately 60.00 Å. Thus, the warped edge is most stable when $\lambda \approx 60.00$ Å. We also find that with the $\lambda < 29.94$ Å, under tension, the warped edge of ribbon transforms to a new configuration with a larger λ. On the other side, with $\lambda > 77.80$ Å, the warped edge tends to turn into a configuration with a smaller λ.

Effect of temperature on warped edge of PG ribbon

As the temperature (T) increases, the thermal-induced fluctuations may become large enough to change the warped edge configuration. To verify this phenomenon, we performed molecular dynamics simulations for the warped edge PG ribbon with the size of 143.69 Å × 359.23 Å and warping number $n = 6$ ($\lambda = 59.86$ Å). Fig. S11 presents the snapshots of PG ribbons during the equilibrium process at different temperatures. We found that with $T \leq 50$ K, there is almost no transformation of the warped edge. However, with $T \geq 50$K, the thermal vibration energy can overcome the energy barrier of the warped edge, leading to the structural transformation of the ribbon.

Figures

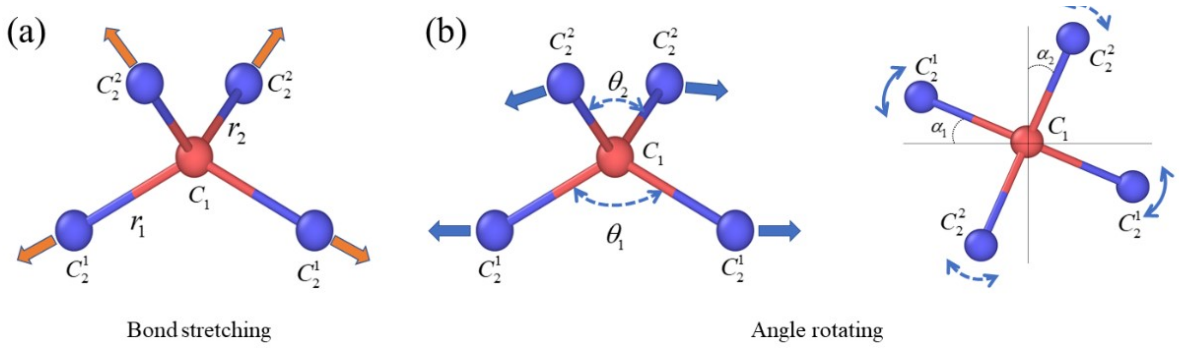

Fig. S1. Two different deformation mechanism of PG (a) bond stretching mechanism in which only bond lengths are elongated while angle θ_1, θ_2, α_1, and α_2 are kept unchanged. (b) angle rotating mechanism.

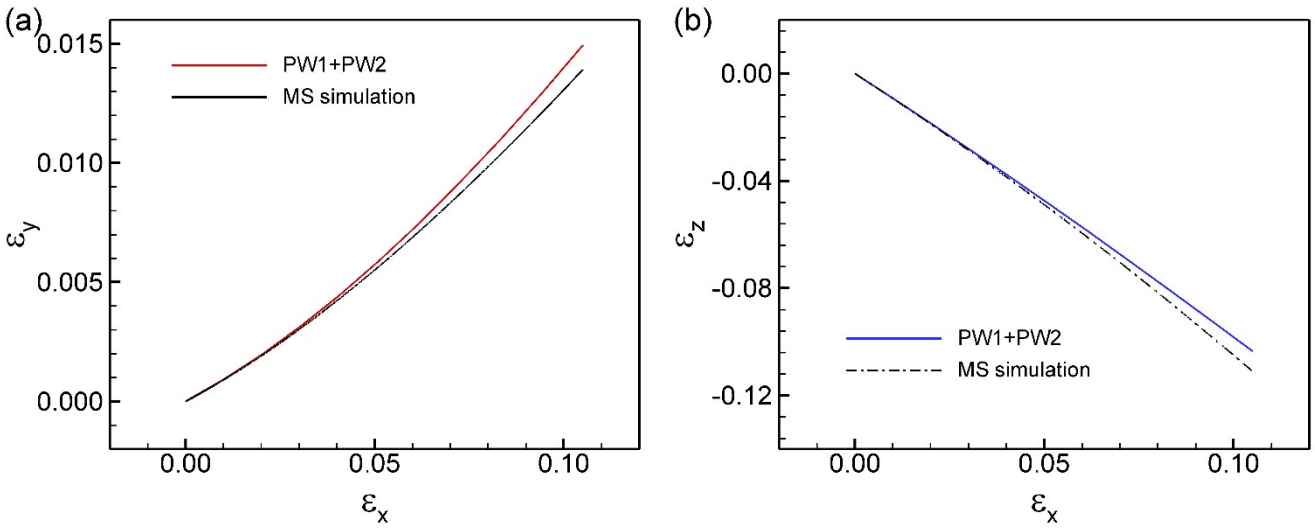

Fig. S2. Deformation in transverse strains (ε_y and ε_z) based on the combination of two pathways and results obtained from molecular statics simulations

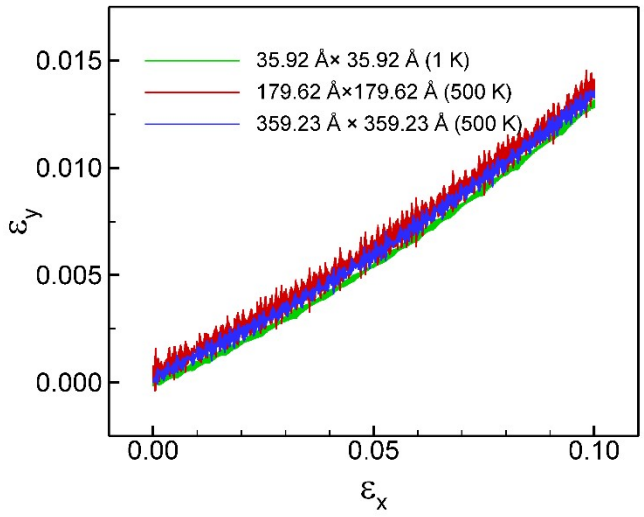

Fig. S3. ε_y - ε_x curve of PG structures with larger size of 179.62 Å×179.62 Å and 359.23 Å × 359.23 Å at different temperatures.

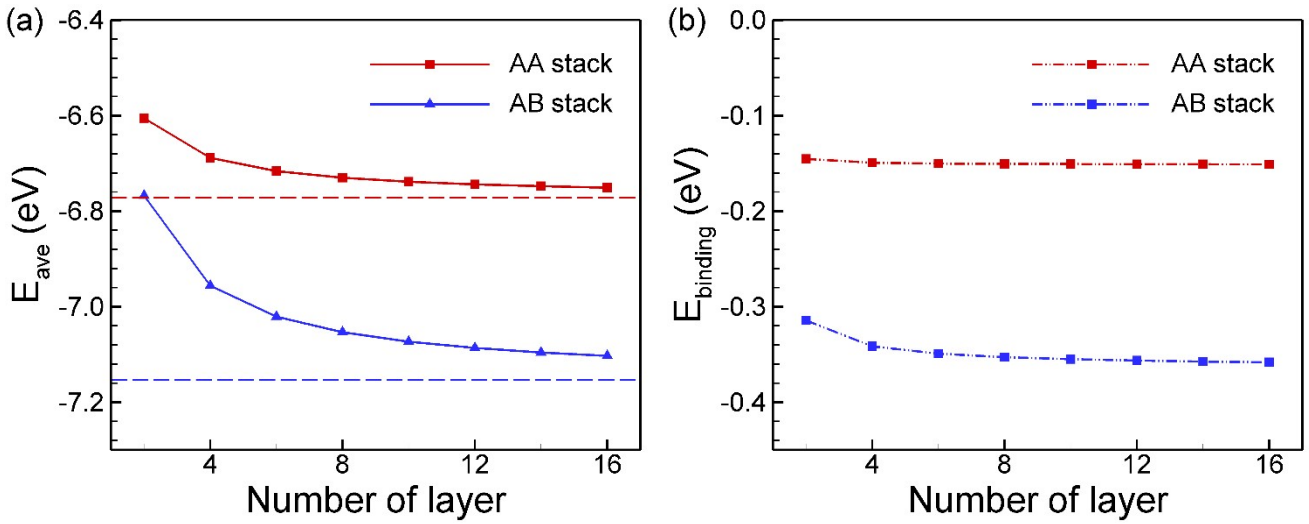

Fig. S4. The dependence of average energy per atom (a) E_{ave} and (b) binding energy on number of layers. $E_{binding}$

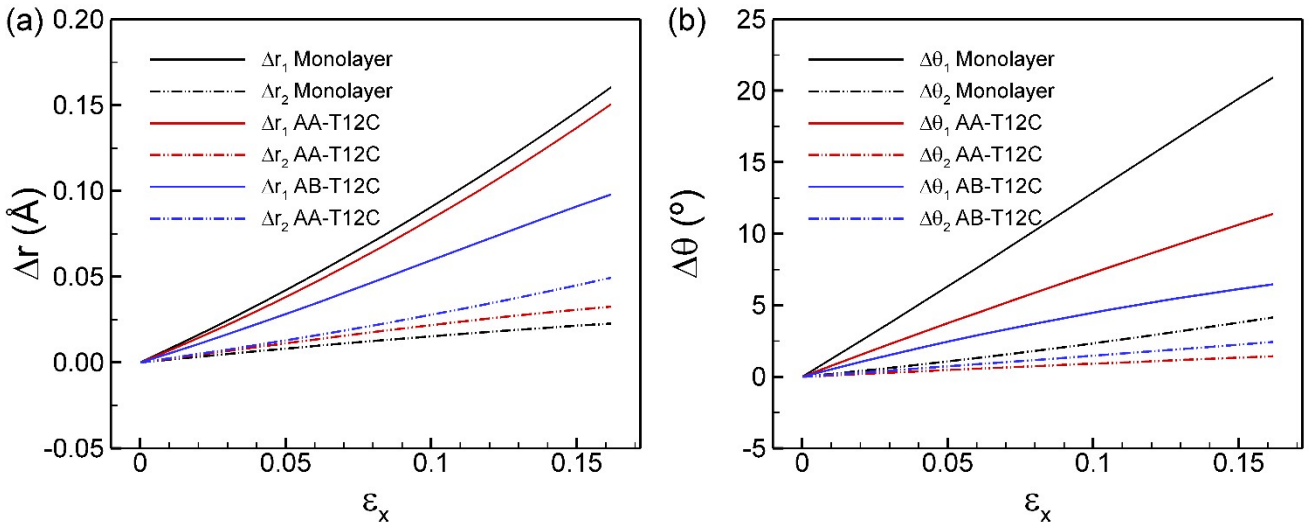

Fig. S5. (a) Variation of bonds lengths (r_1, r_2) and (b) variation angles (θ_1, θ_2) of bulk AA- and AB-T12C as functions of applied strain.

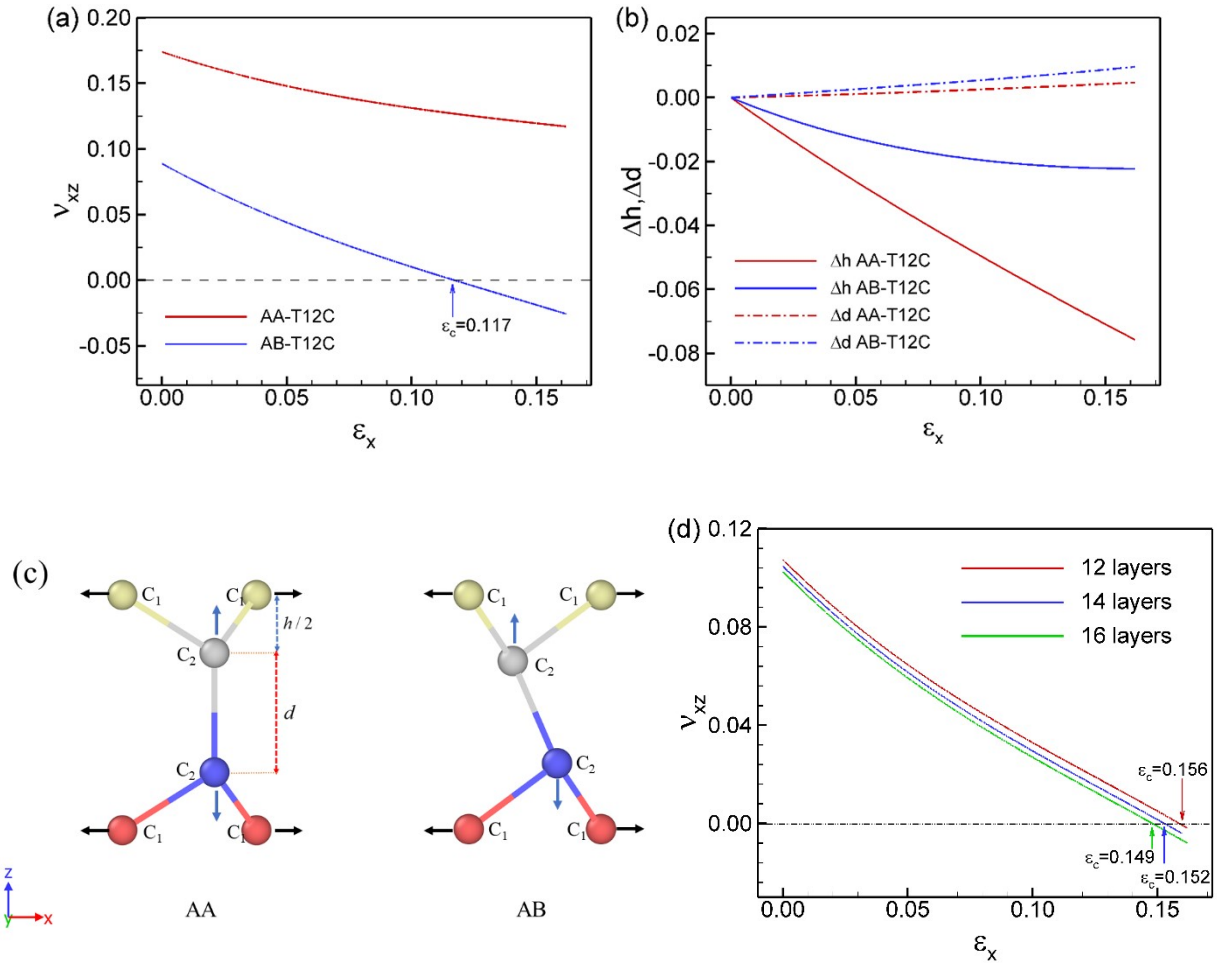

Fig. S6. (a) The out-of-plane Poisson's ratio of bulk AA- and AB-T12C PG as the strain is applied in the *x*-direction. (b) The change of thickness (Δh) of each PG layer and the interlayer distance (Δd) between layers. (c) Deformation direction of atoms as the structure is stretched. (d) The out-of-plane Poisson's ratio of few-layer PG with AB stacking configuration.

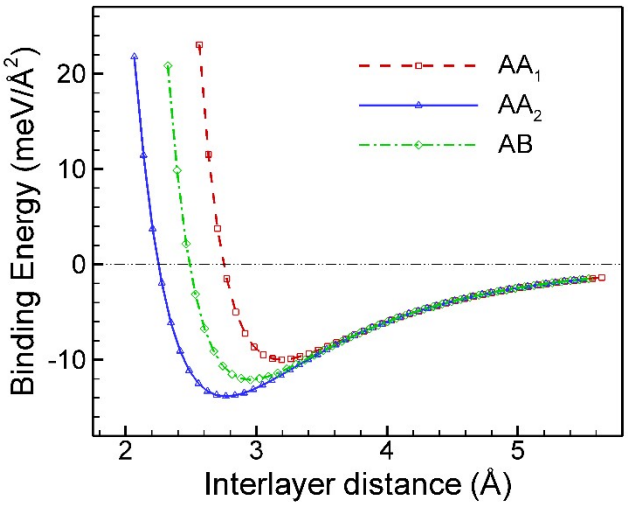

Fig. S7. Binding energy as functions of interlayer distance of bilayer heterostructure PG with difference stacking configurations.

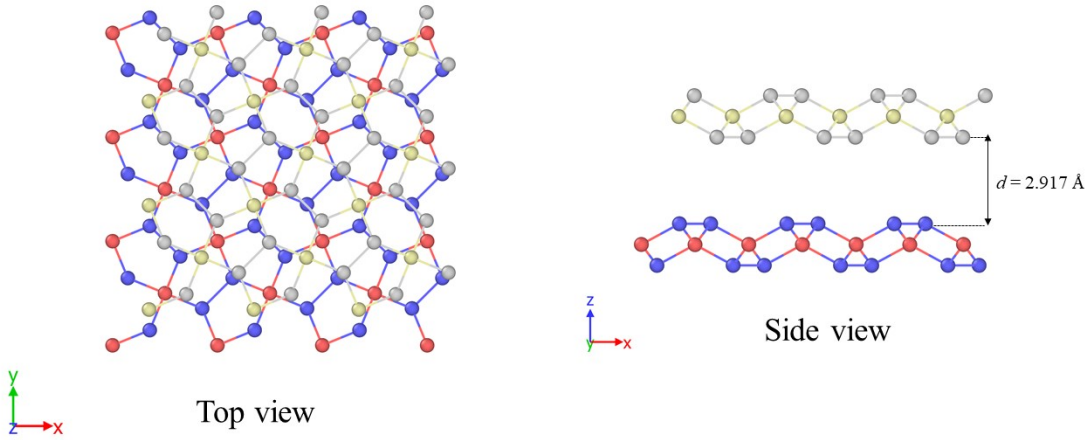

Fig. S8. Transition configuration of heterostructure hAA$_1$ and hAB penta-graphene as the structure is stretched.

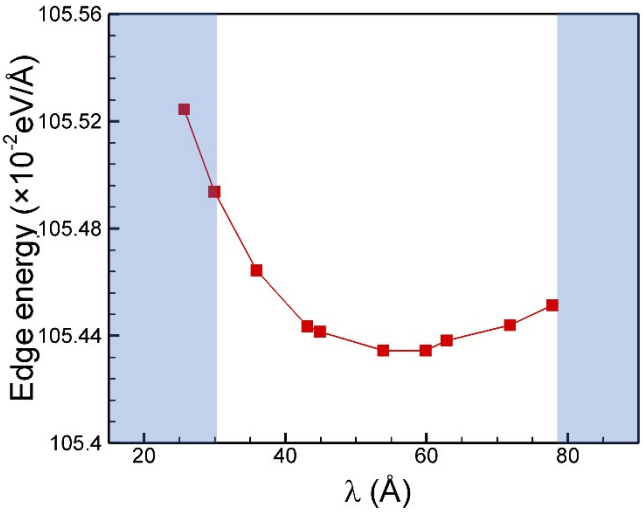

Fig. S9. The relationship between the edge energy of PG ribbon on half wavelength λ. The width of ribbons are with 143.69 Å. The blue shade indicates the unstable of warped edge under tension.

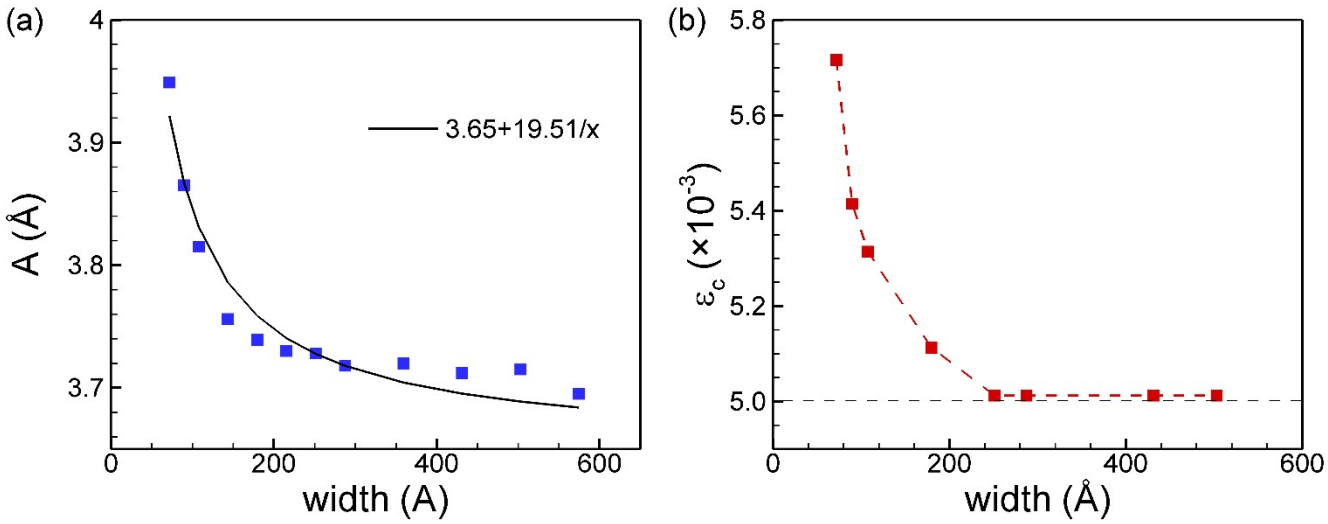

Fig. S10. Dependence of (a) amplitude of warped edge and (b) critical strain on width of PG ribbon.

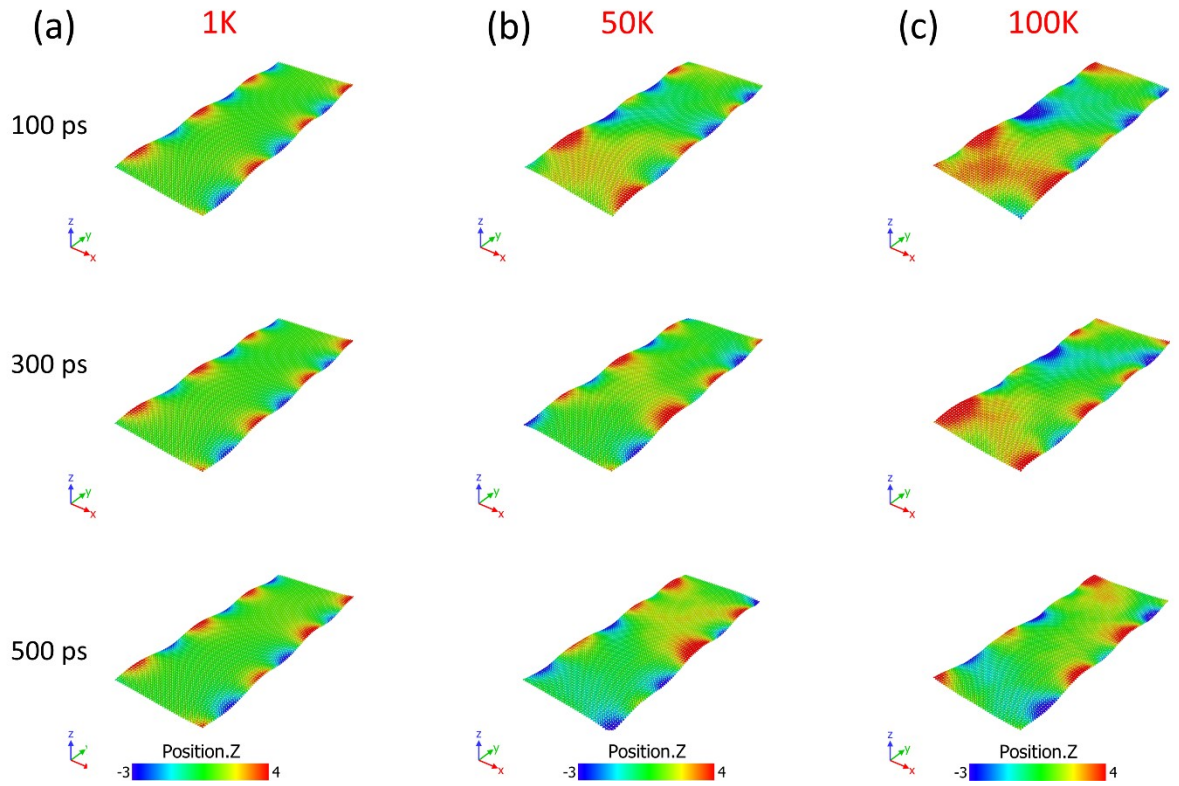

Fig. S11. Snapshots of PG ribbon at different temperatures (a) 1K, (b) 50K, and (c) 100K. The configurations at 100 ps, 300 ps and 500 ps are shown.